

# Isotope Effect in the Superfluid Density of HTS Cuprates: Stripes, Pseudogap and Impurities

J.L. Tallon<sup>1,3</sup>, R.S. Islam<sup>2</sup>, J. Storey<sup>3</sup>, G.V.M. Williams<sup>1</sup> and J.R. Cooper<sup>2</sup>

<sup>1</sup>MacDiarmid Institute, Industrial Research Ltd., P.O. Box 31310, Lower Hutt, New Zealand.

<sup>2</sup>IRC in Superconductivity, Cambridge University, Cambridge CB3 0HE, England. and

<sup>3</sup>School of Chemical and Physical Sciences, Victoria University, Wellington, New Zealand.

(Dated: November 9, 2018)

Underdoped cuprates exhibit a normal-state pseudogap, and their spins and doped carriers tend to spatially separate into 1- or 2-D stripes. Some view these as central to superconductivity, others as peripheral and merely competing. Using  $\text{La}_{2-x}\text{Sr}_x\text{Cu}_{1-y}\text{Zn}_y\text{O}_4$  we show that an oxygen isotope effect in  $T_c$  and in the superfluid density can be used to distinguish between the roles of stripes and pseudogap and also to detect the presence of impurity scattering. We conclude that stripes and pseudogap are distinct, and both compete and coexist with superconductivity.

PACS numbers: 71.10.Hf, 74.25.Dw, 74.62.Dh, 74.72.Dn

High- $T_c$  superconductors (HTS) remain a puzzle. Various correlated states have been identified in HTS including antiferromagnetism, the pseudogap[1], nanoscale spin-charge stripes[2] and, of course, superconductivity (SC). (Here we generalise “stripes” to include possible 2D checkerboard structures[3]). The pseudogap is a nodal energy gap of uncertain origin that appears in the normal-state (NS) density of states (DOS). Its effects can be observed in many physical properties[1, 4]. Several opposing views are still current. One is that stripes play a central role[5], forming the pseudogap correlation[6] and/or mediating the SC pairing. Another is that the NS pseudogap arises from incoherent superconducting fluctuations which set in well above  $T_c$ [7]. Another is that these states are independently competing[8]. Here stripes and pseudogap play a secondary role and SC is mediated by some other pairing boson. An unambiguous test of these opposing views is urgently needed. We show here that isotope effects provide such a test.

The isotope exponent  $\alpha(E)$  in a given property  $E$  is defined as  $\alpha(E) = -(\Delta E/E)/(\Delta M/M)$ , where  $M$  is the isotopic mass and  $E$  may be  $T_c$ , the SC gap parameter,  $\Delta_0$ , the pseudogap energy scale,  $E_g$ , or the superfluid density  $\rho_s = \lambda_{ab}^{-2} = \mu_0 e^2 (n_s/m_{ab}^*)$ . ( $\lambda_{ab}$  is the in-plane London penetration depth,  $n_s$  is the carrier density and  $m_{ab}^*$  is the effective electronic mass for in-plane transport). An isotope effect on  $T_c$  was first discovered in 1950 by Allen *et al.* for Sn[9]. They found  $\alpha(T_c) \approx 0.5 \pm 0.05$  which provided the central clue for the role of phonons in pairing and led 7 years later to the BCS theory of SC[10].

The situation with HTS is more complex. The oxygen isotope effect on  $T_c$  was found[11] to be small, with  $\alpha(T_c) \approx 0.06$ . However, with decreasing doping the effect rises and eventually diverges as  $T_c \rightarrow 0$ [12, 13]. Surprisingly, an isotope effect was also found in the superfluid density[14] (and attempts were made to resolve this into a dominant isotope effect just in  $m^*$ [15, 16]). We will show that both of these unusual effects can be understood in terms of a normal-state pseudogap which competes with

SC[17]. We also predict and confirm an isotope effect in  $\rho_s$  induced by impurity scattering. The isotope effects in  $T_c$  and  $\rho_s$  are mapped as a function of doping in  $\text{La}_{2-x}\text{Sr}_x\text{Cu}_{1-y}\text{Zn}_y\text{O}_4$  and we observe a canonical pseudogap behavior as well as a huge anomalous effect associated with stripes. The clear distinction between these effects shows that the pseudogap and stripe states are distinct and both compete with SC.

An isotope effect,  $\alpha(\rho_s)$ , in the superfluid density is surprising because for a simple BCS superconductor it is rigorously zero. According to Leggett's theorem,  $\rho_s$  is just the total integrated spectral weight of the free carriers i.e. the total carrier density divided by the effective mass[18]. But, when there are strong departures from nearly-free-electron theory this need not be so. We identify two cases for HTS in which an isotope effect in  $\rho_s$  arises: in the presence of (i) impurity scattering, and (ii) a pseudogap.

HTS possess a  $d$ -wave order parameter and in the presence of *impurity scattering* both  $T_c$  and  $\rho_s$  are diminished. The degree to which they are reduced depends upon the magnitude of the scattering rate,  $\Gamma$ , relative to the maximum gap parameter,  $\Delta_0$ , near  $\mathbf{k} = (\pi, 0)$ . In the presence of a competing *pseudogap*, spectral weight removed by the pseudogap is no longer available for the condensate and, again, both  $T_c$  and  $\rho_s$  are diminished. The degree to which they are reduced depends upon the relative magnitudes of the pseudogap and the SC gap. Thus,  $T_c$  and  $\rho_s$  are reduced according to the magnitude of the ratios  $\Gamma/\Delta_0$  for impurity scattering, and  $E_g/\Delta_0$  for a pseudogap. In either case, a relatively small isotope effect in  $\Delta_0$  will necessarily produce enhanced isotope effects in  $T_c$  and  $\rho_s$  which diverge as  $T_c \rightarrow 0$ . Now it has been shown from specific heat, NMR and ARPES that, with increasing doping,  $E_g$  decreases and closes abruptly at a critical doping state,  $p_{crit} = 0.19$  holes/Cu, in the lightly overdoped regime[4]. It follows that the isotope effect in  $\rho_s$  should disappear at critical doping where the pseudogap closes provided that impurity scattering is absent. Our initial task is to quantify these effects.

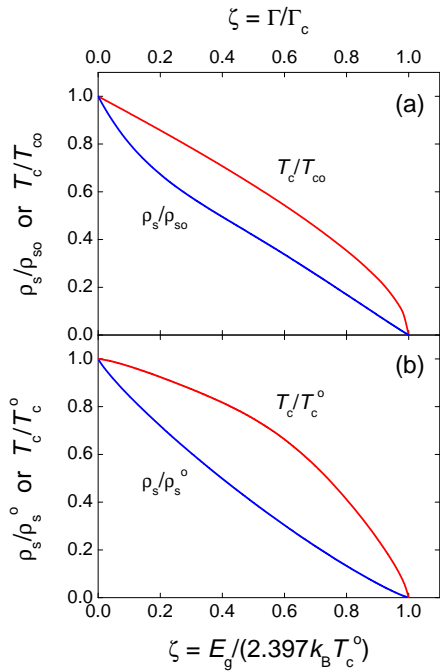


FIG. 1: The fractional suppression of  $T_c$  and superfluid density in a  $d$ -wave SC with (a) unitary-limit impurity scattering and (b) a NS triangular pseudogap with gap energy  $E_g$ .

First, we recall that there is no isotope effect in the pseudogap. We have examined the  $^{89}\text{Y}$  Knight shift in  $\text{YBa}_2\text{Cu}_4\text{O}_8$  using magic angle spinning with extremely narrow linewidths ( $\approx 100$  Hz) and found no isotope effect within the bounds  $\alpha(E_g) \leq 0.01$ [17]. Though not essential, we proceed under the assumption that an isotope effect is confined to the pairing gap,  $\Delta_0$ , and absent from the pseudogap,  $E_g$ . The small isotope effect observed in  $1/T_1T$  in the same compound does not reflect an isotope effect in the pseudogap. Using the enhanced susceptibility formalism it devolves, rather surprisingly, into an isotope effect in the paramagnon frequency[4].

*Theory.* Impurity scattering for a  $d$ -wave order parameter has been investigated by many authors[19, 20]. We summarize the results in Fig. 1(a) which shows the depression of  $T_c$  and  $\rho_s$  as a function of  $\zeta = \Gamma/\Gamma_c$ , where  $\Gamma_c$  is the critical scattering rate for fully suppressing  $T_c$ . The reduction in  $T_c$  follows the standard Abrikosov-Gorkov equation. In the unitary limit, the scattering rate  $\Gamma = n_i/\pi N(E_F)$  where  $n_i$  is the density of scatterers and  $N(E)$  is the NS DOS. Fig. 1(a) shows that  $T_c(\zeta)/T_{c0}$  falls at first slowly then accelerates while  $\rho_s(\zeta)$  falls at first rapidly then slows as  $\Gamma$  grows. We define the functions  $h$  and  $g$  given by  $\rho_s(\zeta)/\rho_{s0} = h(\zeta)$  and  $T_c(\zeta)/T_{c0} = g(\zeta)$ . The isotope effects in  $\rho_s$  and  $T_c$  are

$$\begin{aligned} \alpha(\rho_s) &= -\zeta(h'/h)\alpha(T_{c0}) \\ \alpha(T_c) &= [1 - \zeta(g'/g)]\alpha(T_{c0}) \end{aligned} \quad (1)$$

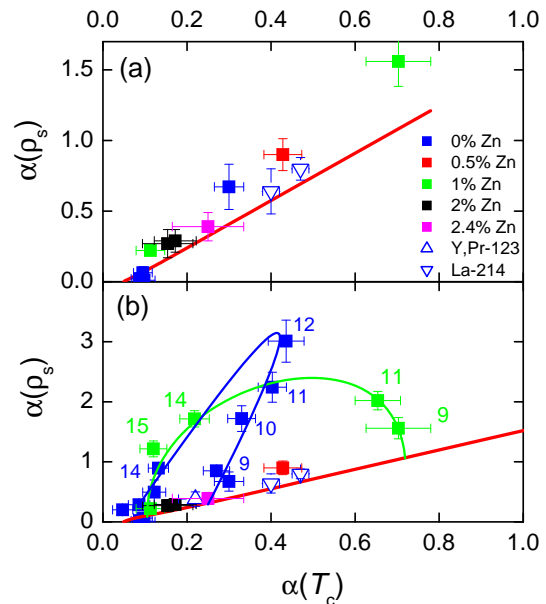


FIG. 2: Oxygen isotope exponent in superfluid density plotted against that in  $T_c$  for  $\text{La}_{2-x}\text{Sr}_x\text{Cu}_{1-y}\text{Zn}_y\text{O}_4$ . Panel (a) shows the calculated (red line) and observed effect of impurities for overdoped ( $x = 0.19, y = 0, 1, 2, 2.4\%$ ) and strongly underdoped ( $x = 0.09, y = 0, 0.5, 1\%$ ) samples. Previous data is also shown (blue down triangles). Panel (b) shows more data for  $0.10 \leq x \leq 0.19$ , with  $y = 0$  (blue squares), and 1% Zn (green squares) and reveals an anomalous deviation from the canonical pseudogap line (red line). Previous data is shown for  $\text{Y}_{1-z}\text{Pr}_z\text{Ba}_2\text{Cu}_3\text{O}_{7-\delta}$  (blue up triangle).

The prime indicates differentiation of  $h(\zeta)$  or  $g(\zeta)$ . Thus

$$\alpha(\rho_s) = -\zeta(h'/h)[1 - \zeta(g'/g)]^{-1}\alpha(T_c) \quad (2)$$

We have shown previously[13, 17] that the isotope effect in  $T_c$  across the entire phase diagram is consistent with an underlying exponent (in the absence of scattering and pseudogap) of  $\alpha(T_{c0}) \approx 0.06$ . The red line in Fig. 2(a) shows  $\alpha(\rho_s)$  plotted versus  $\alpha(T_c)$  using this value. In the absence of impurity scattering  $\alpha(\rho_s) = 0$  and  $\alpha(T_c) = \alpha(T_{c0}) = 0.06$ . This is the left-hand termination of the red line. With increasing scattering both  $\alpha(\rho_s)$  and  $\alpha(T_c)$  rise along the line, and finally diverge as  $\Gamma \rightarrow \Gamma_c$ .

Turning to the pseudogap, specific heat[8] and tunneling measurements[21] show that the pseudogap is non-states-conserving, with an approximately triangular energy dependence, and pinned to the Fermi level,  $E_F$ . We assume therefore a triangular normal-state DOS:

$$\begin{aligned} N(E) &= N_0 \times |E - E_F|/E_g(p); & |E - E_F| < E_g(p), \\ &= N_0; & |E - E_F| > E_g(p). \end{aligned} \quad (3)$$

and solve standard weak-coupling  $d$ -wave BCS expressions to calculate  $T_c$  as a function of  $E_g$ . For this par-

ticular NS DOS  $T_c \rightarrow 0$  as  $E_g \rightarrow 2.397k_B T_c^0$  where  $k_B$  is Boltzmanns constant and  $T_c^0 = T_c(E_g = 0)$ . Fig. 1(b) shows  $T_c$  plotted as a function of  $\zeta = E_g/(2.397k_B T_c^0)$ . As for impurity scattering, the depression in  $T_c$  is slow at first and more rapid as  $\zeta \rightarrow 1$ .

Elsewhere[22] we have calculated the effect of a triangular pseudogap on  $\rho_s$ . The approach is admittedly for a Fermi liquid but we note that the effects we describe are dominated by the nodal regions of the Fermi surface where such a Fermi liquid approach is more likely to be valid.  $\rho_s(\zeta)$  is plotted as a function of  $\zeta$  in Fig. 1(b). This exhibits an initial rapid fall which slows as  $E_g$  grows and  $\zeta \rightarrow 1$ . The overall behavior is qualitatively similar to that shown in Fig. 1(a) for impurity scattering, but differs in detail. We could therefore define new functions  $h(\zeta)$  and  $g(\zeta)$  as above and derive an equation formally identical to eq. (2) to describe the isotope effects in  $\rho_s$  and  $T_c$  associated with the presence of the pseudogap. These equations show that when the pseudogap closes at critical doping we have  $\zeta = 0$  and  $\alpha(\rho_s) = 0$  while  $\alpha(T_c) = \alpha(T_c^0)$ . The resultant curve  $\alpha(\rho_s)$  versus  $\alpha(T_c)$  almost exactly coincides with the red line in Fig. 2(a). If there were an isotope effect in the pseudogap  $\alpha(T_{c0})$  in eq. (1) should be replaced by  $[\alpha(T_{c0}) - \alpha(E_g)]$  and eq. (2) and the red line in Fig. 2 remain unchanged.

*Experimental details.*  $\text{La}_{2-x}\text{Sr}_x\text{Cu}_{1-y}\text{Zn}_y\text{O}_4$  samples were synthesized by solid state reaction at 985°C in air by repeated milling, pelletization and reaction until phase pure as determined by x-ray diffraction. Two small, approximately  $2 \times 2 \times 3 \text{ mm}^3$  bars, were cut from alongside each other at the centre of each of the resultant pellets to ensure, as much as possible, identical pairs. They were isotope exchanged in identical quartz tubes, one charged with  $^{16}\text{O}$  and the other with  $^{18}\text{O}$ , side by side in a furnace. The  $^{18}\text{O}$  gas (from Isotec) was 99% enriched and several exchanges were employed until about 95% exchange was achieved. On the final exchange the samples were slow cooled then annealed for 15 hours at 500°C to ensure oxygenation to full stoichiometry. The degree of exchange was confirmed by Raman measurements of the spectral shifts of the oxygen phonons.

To determine the isotope shifts in  $T_c$  and  $\rho_s$  we carried out field-cooled DC magnetization measurements in the mixed state at 150 Oe. For this regime Zhao and Morris[15] adopted the relation[23]

$$(-M)^{1/2} \propto (r_g/\lambda)[T_c(H)-T] \times [(dH_{c2}/dT)/(2\kappa^2-1)T_c]^{1/2} \quad (4)$$

for the limit, near  $T_c$ , of  $\lambda \gg r_g$ . Here  $r_g$  is the mean radius of the SC grains. These authors showed that this relation could be used to deduce separate isotope effects in  $n_s$  and  $m^*$ . But the algebra was incorrect (see Appendix below). A further problem arises[24] in that, for small particles, this relation does not satisfy the sum rule,  $\mu_0 \int M(H)dH = U_0 \equiv$  the condensation energy. With a mean grain size of  $25\mu\text{m}$  and  $\lambda_{ab}(0)$  ranging from 0.2 to

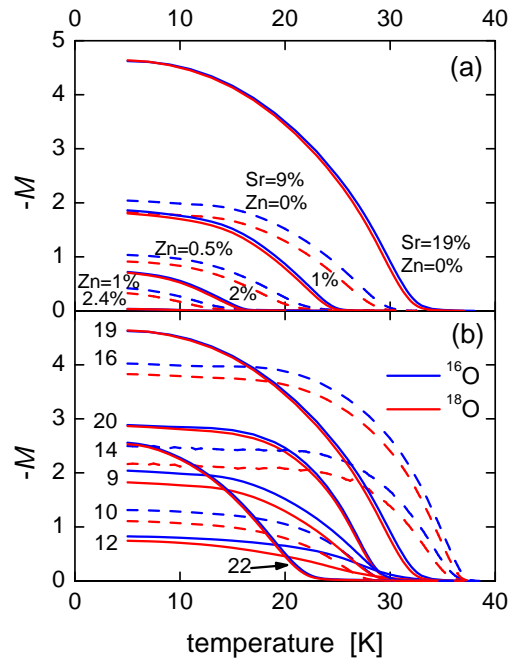


FIG. 3: Magnetization versus  $T$  for  $\text{La}_{2-x}\text{Sr}_x\text{Cu}_{1-y}\text{Zn}_y\text{O}_4$ . Panel (a) shows  $x = 0.19$  with  $y = 0, 1, 2, 2.4\%$  (solid curves) and  $x = 0.09$  with  $y = 0, 0.5, 1\%$  (dashed curves). Panel (b) shows data for Zn-free samples with  $0.09 \leq x \leq 0.22$ .

$0.32\mu\text{m}$ [25], we adopt the limit  $\lambda \ll r_g$  which is clearly satisfied up to a few K below  $T_c$ . This yields

$$-M \propto \lambda^{-2}[1 - T/T_c]. \quad (5)$$

Thus the isotope coefficient in the slope of  $-M(T)$  is given by  $\alpha(\rho_s) - \alpha(T_c)$ . What we report is the partial isotope exponent due to the change in oxygen mass only. We obtained qualitatively similar results with Meissner state measurements at 10 Oe (not shown).

*Results.* We start first with the effect of impurity scattering in the overdoped region  $x = 0.19$  where the pseudogap is absent. Illustrative plots of magnetization versus temperature are shown in Fig. 3(a) for  $y = 0, 1, 2$  and  $2.4\%$  (solid curves). It evident that an isotope effect in  $T_c$  is present in each but that one in  $\rho_s$  is only present in the higher Zn concentrations. Values of  $\alpha(\rho_s)$  are plotted versus  $\alpha(T_c)$  in Fig. 2 (a) (left-hand cluster of blue, green, black and mauve squares) and they are seen to be roughly consistent with the model calculation. The fact that  $\alpha(\rho_s) \rightarrow 0$  as  $y \rightarrow 0$  indirectly shows that any disorder potential present in Zn-free  $\text{La}_{2-x}\text{Sr}_x\text{CuO}_4$  in the overdoped region is too small to present significant scattering and hence  $\alpha(\rho_s) = 0$ . It also seems unlikely that there is any significant phase separation because the domain walls would surely act as scattering centers.

Turning to the heavily underdoped pseudogap region, we show magnetization curves in Fig. 3(a) for  $x = 0.09$

with  $y = 0, 0.5$  and 1% Zn (dashed curves). The resultant  $\alpha(\rho_s)$  versus  $\alpha(T_c)$  values are plotted in Fig. 2(a), shown by the blue, red and green data points to the right. These continue to track up the canonical curve, showing that the pseudogap and impurity scattering have essentially the same effect in such a plot. To this data we add previously-reported[26] values for  $\text{La}_{2-x}\text{Sr}_x\text{CuO}_4$  obtained using muon spin relaxation ( $\mu\text{SR}$ ) with  $x = 0.080$  and  $0.086$  (blue down triangles). The collective data is generally consistent with the model.

Fig. 3(b) shows a selection of illustrative plots of  $M$  vs  $T$  for Zn-free samples with  $x$  ranging from 0.09 to 0.22. It is immediately evident from the low- $T$  values of  $M$  that  $\alpha(\rho_s) = 0$  for all  $x > 0.19$  but becomes non-zero and large as  $x$  falls below 0.19. Values of  $\alpha(\rho_s)$  are plotted against  $\alpha(T_c)$  in Fig. 2 (b) (blue squares) and increasing doping is shown by the arrow. Here, a remarkable anomaly is evident. The overdoped data and the heavily underdoped data lie near the canonical pseudogap line. But near  $x = 0.12$  the data deviates drastically from this canonical behavior. This is presumably due to the presence of charged stripes, inferred from neutron scattering near  $p=1/8$ , which provide strong electronic coupling to the lattice. If the pseudogap itself arose from fluctuating stripes one might expect the anomaly to drive up the canonical line. The huge deviation suggests a fundamentally different behavior and clearly distinguishes stripes from the pseudogap near  $p=1/8$ .

In order to further test this interpretation we examined the effects of non-magnetic Zn substitution. Our expectation was that the combined effects of spin vacancies and the tendency of Zn to enhance the canonical behavior would be to broaden and weaken the anomaly pushing it up the canonical line. Fig. 2(b) shows the effect of 1% Zn substitution (green squares). The contour, indicated by the green curve, confirms our expectations.

Finally, we show by the upward open triangle in Fig. 2(b) recently reported  $\alpha(\rho_s)$  and  $\alpha(T_c)$  data for  $\text{Y}_{1-z}\text{Pr}_z\text{Ba}_2\text{Cu}_3\text{O}_{7-\delta}$  obtained by Khasanov *et al.* using  $\mu\text{SR}$ [27]. For  $z = 0.3$  these authors found  $T_c = 59.3\text{K}$  and we estimate that the doping state is very close to  $p = 0.125$ . And yet the data resides close to the canonical line completely free of the anomalous deviation associated with stripes. It is clear from inelastic neutron scattering studies that the  $\text{YBa}_2\text{Cu}_3\text{O}_{7-\delta}$  compound exhibits a much weaker tendency to stripe formation. Consistent with this we find this sample exhibits essentially stripe-free canonical pseudogap behavior.

We conclude that our results and analysis demonstrate a clear distinction between the canonical effects on the superfluid density arising from the pseudogap and impurity scattering on the one hand and stripe correlations on the other. We achieve this by examining a plot of  $\alpha(\rho_s)$  versus  $\alpha(T_c)$  which is relatively insensitive to the precise details of the NS DOS. Stripes cause a huge deviation from this canonical behavior associated with the

strong electronic coupling to the lattice arising from spatial charge modulation. On the basis of these results we make the important conclusion that stripe and pseudogap correlations are fundamentally different and both compete with each other and with superconductivity.

We acknowledge financial support from the Marsden Fund and the MacDiarmid Institute (JLT, JS and GVMW) and from Trinity College, Cambridge and the Cambridge Commonwealth Trust (RSI).

## Appendix - isotope effect in $m^*$ ?

Several authors[15, 16] have considered the possibility that the isotope effect in  $\rho_s \propto n_s/m^*$  may be resolved into  $\alpha(n_s) - \alpha(m^*)$  and they have sought to determine these two components separately.

Zhao *et al.*[16] investigated the oxygen isotope dependence of the orthorhombic/tetragonal (O/T) transition in  $\text{La}_{2-x}\text{Sr}_x\text{CuO}_4$  and found a null effect. Because the O/T transition temperature is doping dependent they took this to indicate that there was no isotope effect in the carrier concentration and consequently the isotope effect in  $\rho_s$  derives wholly from the isotope effect in  $m^*$  i.e.  $\alpha(\rho_s) = -\alpha(m^*)$ . However, the location of the O/T transition is an ion-size dependent effect not primarily a doping effect and, moreover, there is no simple relationship between the doped hole concentration,  $x$ , and the carrier concentration.

Elsewhere, Zhao and Morris[15] use eq. (5) for 10G measurements to yield a magnetisation slope

$$P_1 \propto r_g^2 n_s / T_c m^*, \quad (6)$$

while for 150G measurements they use eq. (4) from which they deduce

$$P_2 \propto r_g n_s^{5/3} / T_c m^*. \quad (7)$$

Clearly, measurement of the isotope effects in  $P_1$  and  $P_2$  would allow extraction of the individual isotope effects in  $n_s$  and in  $m^*$ . However, eq. (4) does not lead to eq. (7).

To see this we consider the relation[28]

$$H_{c2}(0) = 0.7 T_c [dH_{c2}/dT]_{T_c} = \phi_0 / (2\pi\xi(0)^2). \quad (8)$$

which, on substitution in eq.(4) when  $\kappa = \lambda(0)/\xi(0) \gg 1$ , reduces to eq. (5) and

$$P_2 \propto P_1 \propto n_s / T_c m^*. \quad (9)$$

Thus the isotope effect in  $\rho_s$  cannot be separated into separate contributions from  $\alpha(n_s)$  and  $\alpha(m^*)$  in the way suggested by Zhao and Morris.

---

[1] T. Timusk, B. Statt, Rep. Prog. Phys. **62**, 61 (1999).

- [2] J.M. Tranquada *et al.*, Phys. Rev. Lett. **78**, 338 (1998).
- [3] T. Hanaguri *et al.*, Nature **430**, 1001 (2004).
- [4] J.L. Tallon and J.W. Loram, Physica C **349**, 53 (2000).
- [5] V.J. Emery, S.A. Kivelson, O. Zachar, Phys. Rev. B **56**, 6120 (1997).
- [6] M.I. Salkola, V.J. Emery, S.A. Kivelson, Phys. Rev. Lett. **77**, 155 (1996).
- [7] V.J. Emery, S.A. Kivelson, Nature (London) **374**, 434 (1995).
- [8] J.W. Loram *et al.*, J. Phys. Chem. Solids **59**, 2091 (1998).
- [9] W.D. Allen *et al.*, Nature **166**, 1071 (1950).
- [10] J. Bardeen, L.N. Cooper, J.R. Schrieffer, Phys. Rev. **108**, 1175 (1957).
- [11] B. Batlogg *et al.*, Phys. Rev. Lett. **58**, 2333 (1987).
- [12] J.P. Franck in Physical Properties of High Temperature Superconductors vol. 4, ed by D.M. Ginsburg (World Scientific, Singapore, 1994) 189.
- [13] D.J. Pringle, G.V.M. Williams, J.L. Tallon, Phys. Rev. B **62**, 12527 (2000).
- [14] G-M. Zhao *et al.*, Phys. Rev. B **52**, 6840 (1995).
- [15] G-M. Zhao, D.E. Morris, Phys. Rev. B **51**, 16487 (1995).
- [16] G-M. Zhao, M.B. Hunt, H. Keller and K.A. Müller, Nature **385**, 236 (1997).
- [17] G.V.M. Williams *et al.*, Phys. Rev. Lett. **80**, 377 (1998).
- [18] A.J. Leggett, J. Stat. Phys. **93**, 927 (1998).
- [19] E. Puchkaryov, K. Maki, Eur. Phys. J. B **4**, 191 (1998).
- [20] J.L. Tallon *et al.*, Phys. Rev. Lett. **79**, 5294 (1997).
- [21] V.M. Krasnov *et al.*, Phys. Rev. Lett. **86**, 2657 (2001).
- [22] J.L. Tallon *et al.*, Phys. Rev. B **68** R180501 (2003).
- [23] D.K. Finnemore *et al.*, Phys. Rev. B **35**, 5319 (1987).
- [24] J.R. Clem, Reversible Magnetisation Sum Rule for Small Superconductors, (to be published).
- [25] C. Panagopoulos *et al.*, Phys. Rev. B **67** 220502 (2003).
- [26] J. Hofer *et al.*, Phys. Rev. Lett. **84**, 4192 (2000).
- [27] R. Khasanov *et al.*, J. Phys.: Cond. Mat **15**, L17 (2003).
- [28] N.R. Werthamer, E. Helfand, and P.C. Hohenberg, Phys. Rev. **147** 295 (1966).